Morphology and Thermal Properties of Maleic Anhydride Grafted Polypropylene/Ethylene–Vinyl Acetate Copolymer/ Wood Powder Blend Composites

Dorine Geneth Dikobe, Adriaan Stephanus Luyt

Department of Chemistry, University of the Free State (Qwaqwa Campus), Private Bag X13, Phuthaditjhaba 9866, Republic of South Africa

Received 13 July 2009; accepted 21 October 2009
DOI 10.1002/app.31630
Published online 22 February 2010 in Wiley InterScience (www.interscience.wiley.com).

ABSTRACT: Maleic anhydride grafted polypropylene (MAPP) was blended with ethylene–vinyl acetate (EVA) copolymer to form MAPP/EVA polymer blends. Wood powder (WP) was mixed into these blends at different weight fractions to form MAPP/EVA/WP blend composites. Differential scanning calorimetry (DSC) analysis of the blends showed small melting peaks between those of EVA and MAPP, which indicated interaction and cocrystallization of fractions of EVA and MAPP. The presence of MAPP influenced the EVA crystallization behavior, whereas the MAPP crystallization was not affected by the presence of EVA. Scanning electron microscopy, Fourier transform infrared spectroscopy, and DSC results show that the WP particles in the MAPP/EVA blend were in contact with both the MAPP and EVA phases and that there seemed to be chemical interaction between the different functional groups. This influenced the crystallization behavior, especially of the MAPP phase. The thermogravimetric analysis results show that the MAPP/EVA blend had two degradation steps. An increase in the WP content in the blend composite led to an increase in the onset of the second degradation step but a decrease in onset of the first degradation step. The presence of WP in the blend led to an increase in the modulus but had almost no influence on the tensile strength of the blend. The dynamic mechanical analysis results confirm the interaction between EVA and MAPP and show that the presence of WP only slightly influenced the dynamic mechanical properties. © 2010 Wiley Periodicals, Inc. J Appl Polym Sci 116: 3193–3201, 2010

Key words: blends; calorimetry; composites; fibers; poly(propylene) (PP)

INTRODUCTION

Polypropylene (PP) filled with fillers is of great interest in both research and industry.[1] PP is easily processed, and different types of synthetic and natural fillers can be incorporated into it to form polymer composites. Natural fillers are favored as polymer reinforcers as opposed to synthetic fillers because of the strict environmental policies that force scientists to search for new materials that can substitute for nonbiodegradable composite materials. Wood fiber–plastic composites, in particular, are extensively used in the construction, building, automobile, and infrastructure industries and have created a lot of interest for polymer science research.[2–8]

The addition of natural filler to a polymer is most often used both to reduce production costs and to improve the properties of the thermoplastics, such as rigidity, strength, hardness, and flexural modulus.[3] Natural fillers may cause a slight improvement in a polymer's thermal properties. In a highly filled polymer system, the incompatibility between a polar filler and a nonpolar polymer matrix leads to nonuniformity in the properties because of poor dispersion of the filler in the matrix. To overcome this obstacle, a compatibilizer is usually added. This improves interfacial adhesion between the matrix and filler and may improve the mechanical strength. Maleic anhydride grafted polypropylene (MAPP) is the most commonly used because of the covalent bond that is formed between the anhydride carbonyl and the cellulose hydroxyl groups and also because their good compatibility with the polyolefin matrix.[1–5]

Polymer blending is another method used to improve polymer properties. Polymer blending is favored because it uses conventional technology at a low cost. The main objective of preparing a blend of two or more polymers is not to change the properties of the components drastically but to capitalize on the maximum possible performance of the blend.[9–20] Polymer blend performance depends on the properties of the individual polymers, the

Correspondence to: D. G. Dikobe (dikobedg@qwa.ufs.ac.za).

Contract grant sponsor: National Research Foundation in South Africa; contract grant number: GUN 62017.
Contract grant sponsor: University of the Free State.

© 2010 Wiley Periodicals, Inc.

additives, the preparative method, and the morphology. To obtain a blend with desired characteristics, one must start with a component that already shows that particular characteristic. For example, to improve impact strength, an elastomer must be added; to induce flame retardancy, a nonflammable polymer should be used; and to improve the modulus, a stiffer resin should be incorporated.[15]

PP's applications are often limited because of its low impact strength and Young's modulus properties, particularly at low temperatures and high-temperature loading conditions. One can improve these PP drawbacks considerably by blending in elastomers, particularly ethylene–propylene copolymer, ethylene–propylene–diene terpolymer, or ethylene–vinyl acetate (EVA).[13,16,21] Although PP toughness is improved by blending with elastomers, this causes a decrease in the strength and stiffness. To overcome these limitations, the two approaches for polymer modification can be used together to obtain polymer systems that combine the properties of the blends and fillers. PP has been modified by different fillers and copolymers to produce PP/elastomer/filler ternary composites. The properties of such ternary composites are determined by the composition and characteristics of the components, the phase morphology, and also the relative dispersion of the additive components. In ternary composites containing elastomers and rigid fillers, two extremes in phase structure may occur, where the elastomer and filler particles are dispersed separately in the PP matrix or the rubber encapsulates the filler particles; this results in a low-modulus interlayer between the matrix and the filler.[15,17,22–25]

The purpose of this study was to investigate a MAPP/EVA/wood powder (WP) ternary system. MAPP was chosen because it also has a PP backbone chain, with maleic anhydride (MAH) groups grafted to this backbone. MAPP has been widely used in small quantities for *in situ* or reactive compatibilization of mainly PP and natural fillers.[26]

In this study, MAPP was blended with EVA at equal quantities and mixed with 10, 20, and 30 wt % WP. The effect of the use of MAPP as a component in the blend matrix and not as a compatibilizer was investigated. We were interested in establishing the location and dispersion of WP in these composites and in how this would influence the thermal and mechanical properties of these systems.

EXPERIMENTAL

MAPP, supplied by Pluss Polymers Pvt., Ltd. (India), had a density of 0.91 g/cm^3, a melting point of 165°C, a tensile strength of 24 MPa, and a melt flow index of 55 g/10 min (230°C, 2.16 kg). EVA with 9% vinyl acetate (VA) content, supplied by Plastamid (Elsies River, South Africa) had a density of 0.93 g/cm^3, a melting point of 95°C, melt flow index of 2.5 g/10 min (80°C, 2.16 kg), a tensile strength of 19 MPa, and a 750% elongation at break. Pine WP, or pine saw dust, was obtained from FBW Taurus (Phuthaditjhaba, South Africa). WP, supplied as a light orange powder with a density of 1.5 g/cm^3, was dried at 120°C for 48 h. We obtained particles with sizes of 150 μm or smaller by sieving the dried WP using a laboratory test sieve with a pore size of 150 μm.

The blends and blend composites were weighed according to the required ratios (100/0/0, 0/100/0, 50/50/0, 45/45/10, 40/40/20, and 35/35/30 w/w MAPP/EVA/WP) to make up a total of 38 g (which was the mass required to thoroughly mix the different components in the Brabender Plastograph 50-mL mixer, Duisburg, Germany). The mixing of the samples was done at a temperature of 180°C and a mixing speed of 30 rpm for 15 min. The samples were then melt-pressed at 190°C and 100 bar for 3 min. The pressed samples were allowed to cool at room temperature for 10 min before they were touched to prevent air from penetrating, which would promote the formation of bubbles.

The morphologies of the 50/50 w/w PP/EVA blend and the 40/40/20 w/w PP/EVA/WP composite were examined with a Shimadzu (Kyoto, Japan) SSX-550 Superscan scanning electron microscope. The samples were immersed in liquid nitrogen to ensure perfect breakage. The fractured surface was sputter-coated with gold dust (60 nm) before viewing. The EVA in the 50/50 w/w PP/EVA blend and the 40/40/20 w/w PP/EVA/WP blend composite was extracted using *n*-heptane for 24 h. The residues from these samples were dried in an oven at 50°C for 24 h and analyzed in the scanning electron microscope.

Fourier transform infrared (FTIR) microscopy was performed with a PerkinElmer Precisely Multiscope (Wellesley, MA). Very thin samples were placed under the microscope, and microscope photos and FTIR spectra of the desired areas were collected. The samples were scanned with a PerkinElmer Spectrum 100 FTIR spectrometer over the range 400–4000 cm^{-1} at a resolution of 4 cm^{-1}.

Differential scanning calorimetry (DSC) analyses were carried out in a PerkinElmer DSC7 differential scanning calorimeter under flowing nitrogen (20 mL/min). Two methods were used. In the first method, samples with masses of approximately 7.5 mg were heated from 25 to 190°C at a rate of 10°C/min to eliminate the thermal history, cooled to 25°C at 10°C/min, and reheated under the same conditions. The second method was the same as the first method except that cooling was done at 2°C/min. Three different samples were analyzed for each

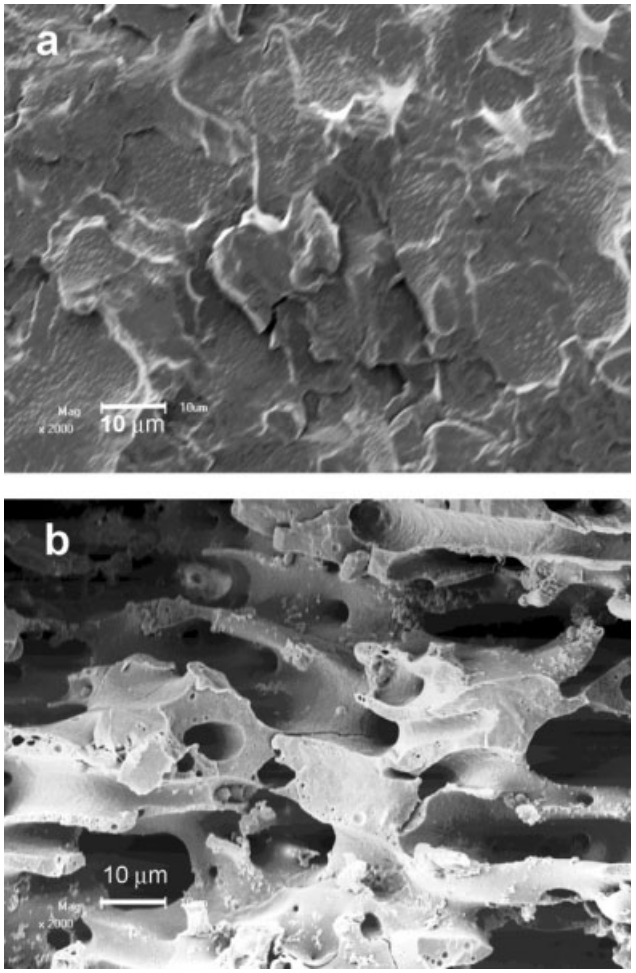

Figure 1 SEM photos of the fracture surfaces of 50/50 w/w MAPP/EVA (a) before solvent extraction of EVA and (b) after extraction (2000× magnification).

composition, and the melting and crystallization data were obtained from the second scan. A statistics computer program was used to eliminate out-of-range values, and the means and standard deviations of the accepted values are reported.

For dynamic mechanical analysis (DMA), rectangular samples 50 × 12.5 × 2 mm^3 in size were used. A PerkinElmer Diamond DMA was used for the evaluation of the storage modulus, loss modulus, and mechanical damping factor. The temperature range over which the properties were measured was −100 to 100°C at a heating rate of 5°C/min under 30 mL/min flowing nitrogen. The tests were carried out at a frequency of 1 Hz.

Thermogravimetric analysis (TGA) was carried out with a PerkinElmer TGA7 thermogravimetric analyzer. Samples with masses of approximately 10 mg were heated from 50 to 600°C at a heating rate of 20°C/min under flowing nitrogen (20 mL/min).

Tensile testing was performed under ambient conditions on a Hounsfield (Tinius Olsen, Salfords, Surrey, UK) H5KS universal tester at a crosshead speed 50 mm/min. Tensile test specimens (gauge length = 24 mm, width = 5 mm, thickness = 2 mm) were prepared with a dumbbell-shaped hollow punch. Six samples per composition were analyzed. A statistics computer program was used to eliminate out-of-range values, and the means of the accepted values are reported.

RESULTS AND DISCUSSION

Scanning electron microscopy (SEM) microphotos of the fractured surface of the MAPP/EVA blend before and after extraction are presented in Figure 1. In our previous study of the morphology and properties of PP/EVA/WP blend composites, it was not possible to see separate PP and EVA phases on the SEM photo of the 50/50 w/w PP/EVA blend.[17] The same observation was reported by Mihaylova et al.[18] and Gupta et al.,[19] who used SEM to study the structures of PP/EVA blends and who found it difficult to distinguish between the two phases when PP and EVA were blended in equal quantities. It was

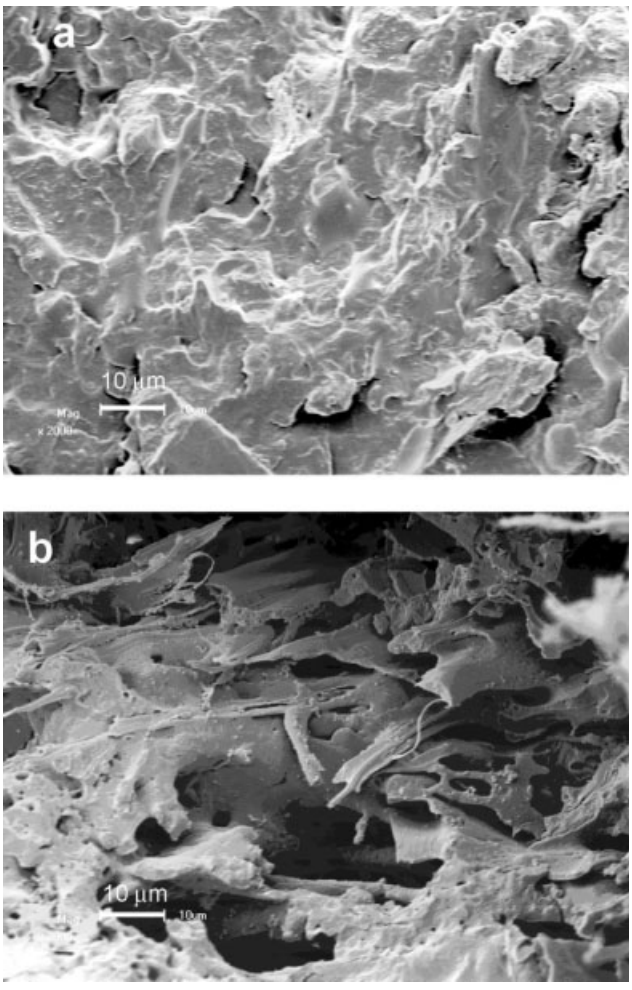

Figure 2 SEM photos of the fracture surfaces of 40/40/20 w/w MAPP/EVA/WP (a) before solvent extraction of EVA and (b) after extraction (2000× magnification).

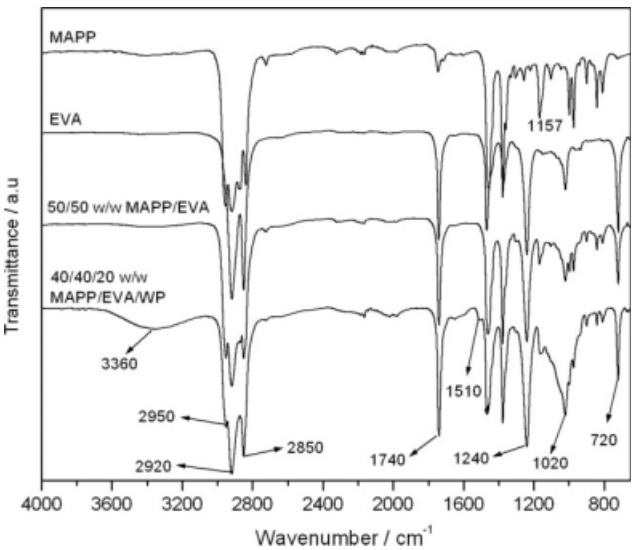

Figure 3 FTIR spectra of pure EVA, pure MAPP, the MAPP/EVA blend, and the MAPP/EVA/WP blend composites (before solvent extraction of EVA).

also not possible to distinguish between the EVA and MAPP phases in the SEM photo of our blend [Fig. 1(a)]. However, the SEM photo of the sample after solvent extraction of EVA clearly showed the presence of a cocontinuous morphology [Fig. 1(b)].

Figure 2 shows the fractured surfaces of the 40/40/20 w/w MAPP/EVA/WP blend composites before and after extraction. The SEM photo of the blend composite before extraction did not conclusively show any morphological features [Fig. 2(a)]. The SEM photo of the blend composite after extraction clearly showed the WP particles in contact with MAPP and with void areas around them where the extracted EVA was situated. This was possible when one considers that MAPP had MAH groups and EVA had —C=O functional groups that could interact/react with the —OH groups in WP. This finding was also reported by Xanthos et al.,[27] who studied compatibilized PP/PET blends and who showed that the hydroxyl group of poly(butylene terephthalate) could react with functional groups such as MAH. In our previous study on PP/EVA/WP blend composites, we reported that there was an interaction between EVA and WP, mainly due to the carboxylic group of EVA and the hydroxyl group of cellulosic WP.[17]

Figure 3 shows the FTIR spectra of EVA, MAPP, the MAPP/EVA blend, and the 40/40/20 MAPP/EVA/WP blend composite. EVA and MAPP had similar functional groups, and therefore, it was quite a challenge to identify the characteristic peaks of MAPP and EVA in the MAPP/EVA blend. Kim et al.[12] studied the reactive compatibilization of a poly(butylene terephthalate)/EVA blend by MAH. They reported that identification of characteristic peaks of MAH, which was grafted on EVA, was difficult because the EVA and MAH possessed a similar —C=O functional group. However, they concluded that there was a reaction between EVA and MAH forming EVA-*g*-MAH.[12] MAPP and EVA, respectively, had four and two distinctive characteristic peaks around 2850–2950 cm^{-1} due to C—H stretching. The peak representing the vibration of the —C=O ester of the carboxyl group appeared at 1740 cm^{-1} in pure EVA, pure MAPP, and the MAPP/EVA blend. Huerta-Martinez et al.[11] investigated a PP–ethylene–propylene/poly(ethylene vinyl acetate) system and reported that above 40% EVA, vibrations at 997 and 1153 cm^{-1} were particularly associated with the crystalline/amorphous bands of EVA, and therefore, their change was associated with an interaction occurring in either of these two phases. A similar trend was observed in our MAPP/EVA system, where there was a change in the vibrations at 1157 cm^{-1} and below for the MAPP/EVA blend in comparison to the pure EVA and pure MAPP spectra. The presence of WP in the blend composite was indicated by a strong, broad —OH functional group stretching vibration around 3360 cm^{-1} and an —OH bend vibration at 1020 cm^{-1}. All of the other peaks were consistent with the peaks observed in the MAPP/EVA blend. This observation supported the SEM observation of the WP being evenly dispersed in both polymers in the blend.

The FTIR spectra of the MAPP/EVA blend and the MAPP/EVA/WP blend composite after solvent extraction of EVA are presented in Figure 4. The spectrum of the extracted MAPP/EVA blend was dominated by the MAPP stretching vibrations; this indicated that most of the EVA was extracted by

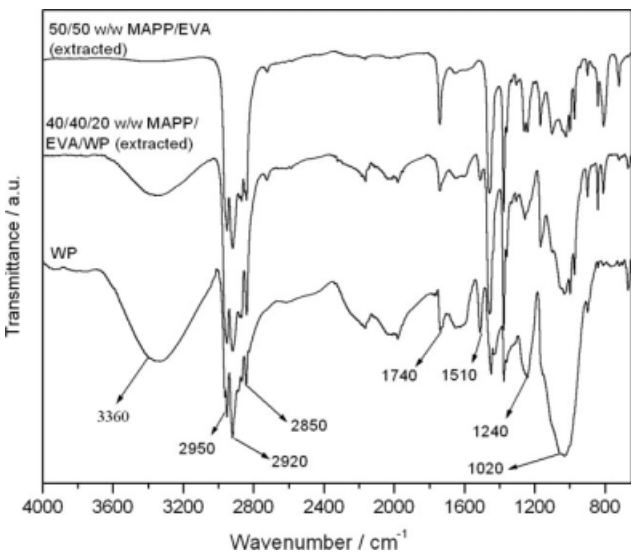

Figure 4 FTIR spectra of WP, the MAPP/EVA blend, and the MAPP/EVA/WP blend composites (after solvent extraction of EVA).

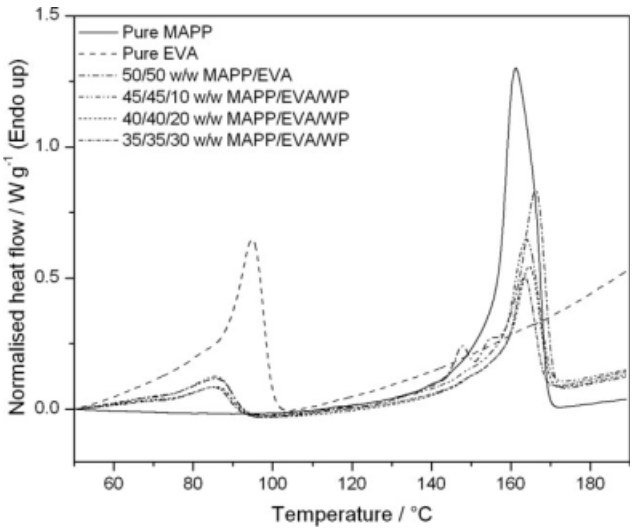

Figure 5 DSC heating curves of pure EVA, pure MAPP, and the MAPP/EVA/WP blend composites (after cooling at 10°C/min).

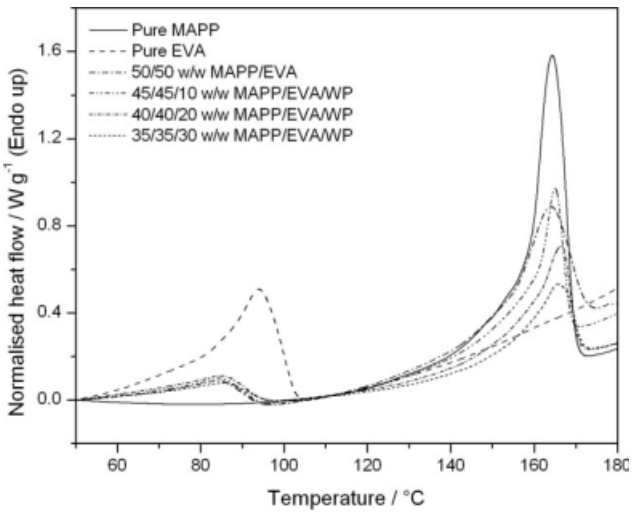

Figure 6 DSC heating curves of pure EVA, pure MAPP, and the MAPP/EVA/WP blend composites (after cooling at 2°C/min).

n-heptane. This observation was supported by a decrease in the EVA characteristic peaks at 1740, 1240, and 720 cm^{-1} when we compared the MAPP/EVA blend spectra before and after extraction. The spectrum of the extracted MAPP/EVA/WP composite had a strong, broad —OH stretching vibration around 3360 cm^{-1} and an —OH bending vibration at 1020 cm^{-1}. Another peak at 1510 cm^{-1}, characteristic of cellulose, was observed in the spectra of both WP and the WP blend composite but was absent in all of the other spectra. The other remaining peaks were more closely related to MAPP and not EVA. This observation was in line with the SEM photos [Fig. 2(b)], which showed some WP still in close contact with MAPP, whereas the other WP was located in void areas from where EVA was extracted.

Figures 5 and 6 show the DSC curves of the MAPP/EVA blend and its WP composites cooled at 2 and 10°C/min. In both cases, pure EVA and pure MAPP showed single endothermic peaks at 95 and 164°C. After 50/50 w/w MAPP/EVA was cooled at 10°C/min, the EVA melting peak temperature decreased to 85°C, and that of MAPP increased slightly to 165°C. It was interesting to see that multiple melting peaks existed between the melting peaks of EVA and MAPP (Fig. 5). However, after the same blend was cooled at 2°C/min, only two endothermic melting peaks at 85°C (EVA) and 164°C (MAPP) were observed (Fig. 6). The enthalpy values for the two components also showed interesting changes (Tables I and II). That of EVA showed a significant reduction compared to the calculated value (which we calculated by taking into account the fraction of EVA in the blend and assuming that blending did not change the crystallization behavior of the polymer). On the other hand, there was a slight increase in the melting enthalpy of the MAPP component compared to the calculated value. All of these observations were indications that there was some cocrystallization of EVA and MAPP. It looked as if some EVA chains cocrystallized with the MAPP chains, but a small fraction of the cocrystallized chains seemed to form a separate crystalline phase during fast cooling because of the interaction between the two components. At a slow cooling rate, the tendency to phase separate was larger than the interactive forces because the intramolecular interaction in the pure EVA and MAPP crystals was probably

TABLE I
DSC Melting Data for the Pure MAPP, Pure EVA, and Their Blend Composites (10°C/min Cooling)

	T^{Peak} (°C)		ΔH^{obs} (J/g)		ΔH^{calc} (J/g)	
MAPP/EVA/WP (w/w)	EVA	MAPP	EVA	MAPP	EVA	MAPP
100/0/0	–	164.1 ± 4.1	–	75.3 ± 3.8	–	75.3 ± 3.8
0/100/0	94.9 ± 5.7	–	50.6 ± 1.2	–	50.6 ±1.2	–
50/50/0	85.2 ± 3.8	165.8 ± 5.9	10.5 ± 0.2	38.3 ± 3.1	25.6 ± 2.3	37.7 ± 1.7
45/45/10	84.8 ± 4.3	164.2 ± 4.5	9.8 ± 0.4	36.3 ± 2.5	22.7 ± 1.8	33.8 ± 1.6
40/40/20	84.9 ± 3.7	164.8 ± 4.8	8.4 ± 0.2	33.5 ± 2.9	20.2 ± 1.7	30.1 ± 1.1
35/35/30	85.1 ± 2.8	163.8 ± 3.1	8.1 ± 0.6	29.6 ± 2.8	17.7 ± 0.8	26.3 ± 1.7

TABLE II
DSC Melting Data for the Pure MAPP, Pure EVA, and Their Blend Composites (2°C/min Cooling)

	T^{Peak} (°C)		ΔH^{obs} (J/g)		ΔH^{calc} (J/g)	
MAPP/EVA/WP (w/w)	EVA	MAPP	EVA	MAPP	EVA	MAPP
100/0/0	–	164.5 ± 6.9	–	77.3 ± 3.8	–	77.3 ±3.8
0/100/0	93.7 ± 5.2	–	57.2 ± 3.2	–	57.2 ± 3.2	–
50/50/0	85.4 ± 3.5	163.1 ± 5.4	11.7 ± 1.1	40.1 ± 4.1	28.6 ± 2.6	38.6 ± 2.4
45/45/10	85.3 ± 2.4	165.1 ± 5.8	11.3 ± 0.7	39.6 ± 3.2	25.7 ± 1.9	34.7 ± 2.3
40/40/20	84.9 ± 3.7	166.4 ± 7.3	10.9 ± 0.9	37.6 ± 3.8	22.9 ± 1.7	31.0 ± 2.1
35/35/30	84.7 ± 2.8	165.7 ± 4.9	10.3 ± 1.3	32.9 ± 2.7	20.0 ± 0.9	27.1 ± 1.9

T^{peak} is the peak temperature of melting.

stronger than the intermolecular interaction between MAPP and EVA, and if enough time was given for the crystallization process to occur, separate crystallization was favored above cocrystallization. The sum of the melting enthalpies of the polymers in the blend was smaller than the sum of the calculated melting enthalpies, which indicated that a significant part of the EVA did not crystallize at all. It seemed as if the interaction between the MAPP and EVA chains immobilized the EVA and inhibited its crystallization. This was supported by Xu et al.,[28] who reported that in a polymer blend, cocrystallinity occurs when the low-melting polymer lamellae are incorporated into the high-melting polymer lamellae. The miscibility of the molten phases in the blend and the crystallization rate strongly depend on the molecular structure of the polymers, such as the branch content, molecular shape, and molecular weight. In our case, the linear parts of the EVA seemed to be incorporated into the MAPP crystals.

Similar results were reported by Fonseca and Harrison[10] on the cocrystallization of low-density polyethylene (LDPE) and high-density polyethylene (HDPE) in 90/10 w/w LDPE/HDPE blends. This blend was crystallized under a variety of cooling conditions (slow cooling, intermediate cooling, and quenching). The intermediate peak was clearly observed after rapid cooling, and it shifted toward the highest temperature endotherm (HDPE melting) as the cooling rate was reduced. At the slowest cooling rate, the intermediate peak disappeared. They explained this as being the result of the formation of cocrystallites from HDPE and LDPE, which occurred during fast-cooling crystallization because of the slower diffusion and segregation of HDPE from LDPE. The cocrystal consisted of material normally associated with the higher temperature portion of LDPE and the lower temperature tail of HDPE. These findings were supported by temperature rising elution fractionation (TREF) analysis, which showed that the cocrystalline material contained both a fraction of the original LDPE and a fraction of HDPE.[10]

The addition of WP led to an increase in the crystallinity of both polymers because the difference between ΔH^{obs} and ΔH^{calc} (where ΔH^{obs} is the experimentally determined melting enthalpy from the DSC melting peak areas, and ΔH^{calc} is calculated from the weight fraction of EVA or MAPP in the sample, and the ΔH^{obs} of pure EVA or MAPP) decreased with increasing WP content (Tables I and II). Because WP was in contact with both polymers and because it seemed as if there was an interaction between WP and the polymers, the WP particles probably acted as nucleation agents for the crystallization of EVA and MAPP. The presence of WP in the blend reduced the direct contact and interaction between EVA and MAPP and, therefore, inhibited the formation of the cocrystals, which gave rise to smaller melting peaks between those of EVA and MAPP (Fig. 5).

For both the 10 and 2°C/min cooling rates, generally, there was a decrease in the crystallization temperature (T_c) of EVA in the blend and composites, whereas T_c of the MAPP component remained constant in the MAPP/EVA blend (Figs. 7 and 8). The presence of MAPP seemed to influence the crystallization of EVA, whereas the MAPP crystallization

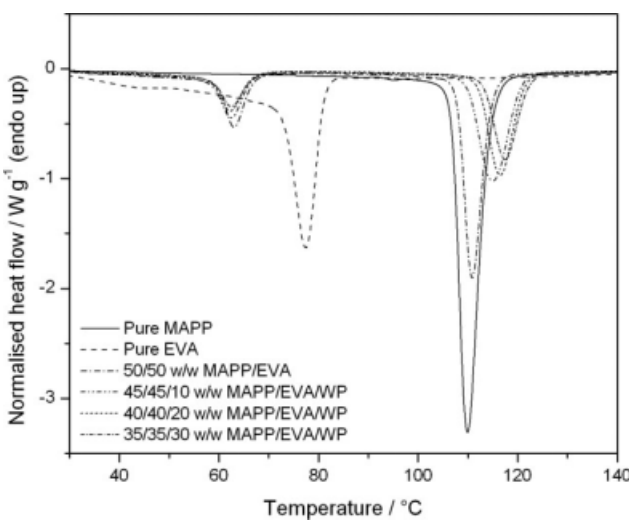

Figure 7 DSC cooling curves of pure EVA, pure MAPP, and the PP/EVA/WP blend composites (cooling rate = 10°C/min).

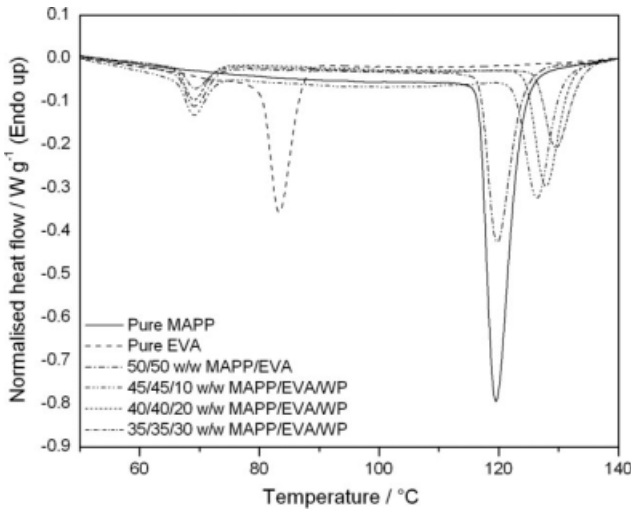

Figure 8 DSC cooling curves of pure EVA, pure MAPP, and the PP/EVA/WP blend composites (cooling rate = 2°C/min).

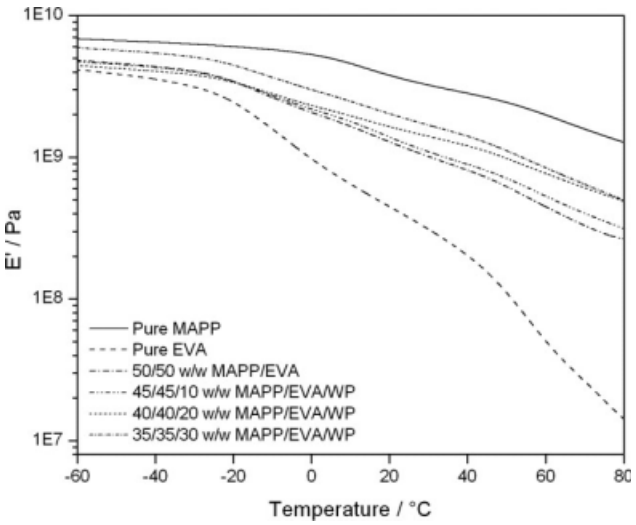

Figure 9 Storage modulus (E') as function of temperature of pure EVA, pure MAPP, the MAPP/EVA blend, and the MAPP/EVA/WP blend composites.

was not affected by the presence of EVA. This was possible because T_c of EVA was lower than that of MAPP, and therefore, the presence of MAPP crystals was likely to hinder EVA crystallization. The presence of WP in the blend caused an increase in MAPP T_c, whereas T_c of the EVA part remained the same for the blend and composites, regardless of the amount of WP present. The fact that the presence of WP did not change EVA T_c was probably due to the fact that WP was mainly situated in the amorphous regions of EVA. On the other hand, WP seemed to act as a nucleating agent for the crystallization of MAPP.

The DMA storage modulus and damping factor curves of the different samples are presented in Figures 9 and 10. EVA had lower storage moduli than MAPP over the whole temperature range, and the difference became more significant with increasing temperature (Fig. 9). The blend had storage moduli between those of pure EVA and pure MAPP over the whole temperature range, and the presence of WP in the blend composites did not seem to significantly change these values, although the WP-containing composites had slightly higher values because of the higher stiffness of cellulose and the interaction between WP and the polymers in the blend. The damping properties of the material give the balance between the elastic and viscous phases in a polymeric structure. The damping behavior of the composites in the transition region is influenced by the mechanical relaxation of the matrix and the fiber, the interface between the fiber and the matrix, and the fiber loading and fiber length.[20] The damping factor curve of EVA showed a β transition at about 0°C and an α transition at about 58°C (Fig. 10). The β transition corresponded to the glass transition of EVA. MAPP had a β-transition peak at about 13°C. Jayanarayanan et al.[20] and Qui et al.[7] reported that the β transition around 10°C corresponded to the glass transition of the amorphous regions in PP. The MAPP/EVA blend showed the β-transition peaks of both EVA and MAPP, whereas the α transition of EVA at about 58°C was absent. The disappearance of this transition indicated that the interaction between MAPP and EVA and its negative influence on EVA crystallization reduced the lamellar shear in EVA to such an extent that the α transition was no longer visible. In our previous study on the PP/EVA/WP system, we reported that the damping factor curve of the PP/EVA blend showed all the transitions observed in pure PP and pure EVA, which indicated complete immiscibility of the two components.[17] However, when WP was

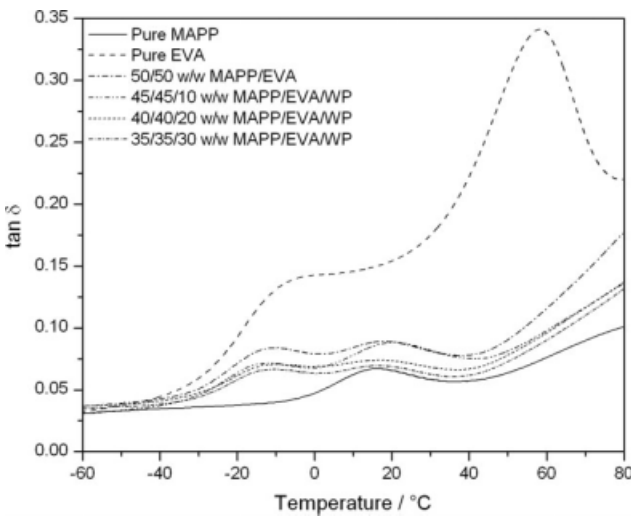

Figure 10 Damping factor as function of temperature of pure EVA, pure MAPP, the MAPP/EVA blend, and the MAPP/EVA/WP blend composites.

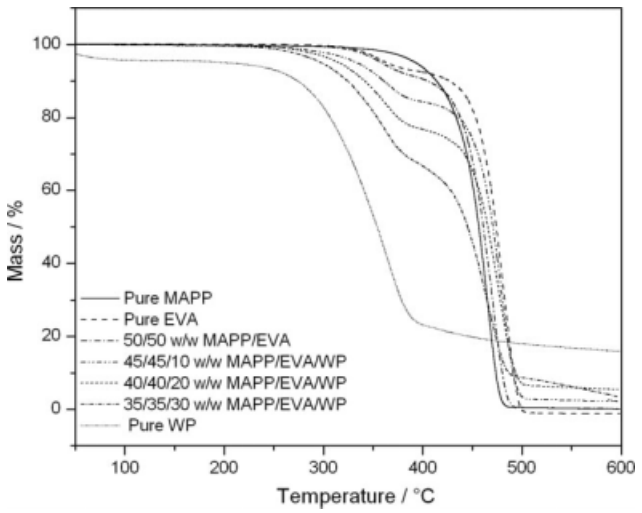

Figure 11 TGA curves of pure EVA, pure MAPP, pure WP, the MAPP/EVA blend, and the MAPP/EVA/WP blend composites.

present, the α transition disappeared because of the interaction between EVA and WP, which gave rise to reduced chain mobility and interlamellar shear. In this case, there was not much difference between the damping factor curves of the blend and the composites because of strong interactions, even in the absence of WP.

The TGA and the derivative TGA curves of the different samples are shown in Figure 11. EVA showed two degradation steps, whereas MAPP had only one degradation step. The first degradation step (ca. 190°C) of EVA was related to the removal of the VA group, whereas the second degradation step was due to the degradation of the polyethylene backbone.[13] The MAPP/EVA blend had two degradation steps. The first one was related to the degradation of the VA group in the EVA part of the blend, whereas the second degradation was due to the simultaneous degradation of MAPP and the EVA polyethylene backbone. The blend composites also had two degradation steps. The first one was attributed to the simultaneous degradation of WP and the deacetylation of EVA, whereas the second one was due to the degradation of the EVA backbone and MAPP.[17]

An increase in WP led to the thermal stabilization of the second degradation step and a decrease in the temperature of the first degradation step. The thermal stability of the second degradation step may have been due to the interfacial interaction between WP, EVA, and MAPP. Similar results were reported by Qui et al.[8] for their study of the structure and properties of composites of highly crystalline cellulose with PP. They reported that no significant change was observed in the thermal stability of PP in the presence of cellulose because of the lack of compatibility between the two. In the presence of a MAPP compatibilizer, however, the thermooxidative stability of the PP/cellulose composites was enhanced because of the improvement in interfacial interaction between the PP matrix and the cellulosic filler. We[17] reported a delay in the PP/EVA thermal degradation and attributed it to the retardation of the evaporation of volatile degradation products due to the char formed during the first degradation step. Peeterbroeck et al.[29] and Joseph et al.[30] reported that EVA and PP became more thermally stable in the presence of clay and sisal fiber, respectively, mainly because of a decrease in the rate of evolution of the volatile products. Duquesne et al.[31] reported that the second degradation step in EVA/nanoclay systems occurred at a higher temperature in the presence of clay because of a diffusion effect, which limited the emission of the gaseous degradation products and resulted in an increase in the thermal stability of the second degradation step of EVA. The decrease in the thermal stability of the components associated with the first degradation step with an increase in WP was due to the fact that cellulosic fillers are considered to be less thermally stable and, hence, promote the degradation of the blend composites.[32,33]

The tensile properties of the blend and composites as a function of filler content are presented in Table III. Blending the MAPP (modulus = 472 MPa) with EVA (modulus = 38 MPa) caused an increase in the Young's modulus of rubbery EVA because of the addition of crystalline MAPP, which reduced the flexibility of the EVA chains. The additions of the fillers influence the mechanical

TABLE III
Mechanical Properties of the MAPP/EVA/WP Blend Composites

MAPP/EVA/WP (w/w)	Tensile modulus (MPa)	Elongation at break (%)	Tensile strength (MPa)
100/0/0	472 ± 15	15.7 ± 1.2	24.9 ± 2.7
0/100/0	38 ± 1	535 ± 12	9.9 ± 0.5
50/50/0	258 ± 4	23.0 ± 0.1	12.6 ± 0.2
45/45/10	308 ± 3	13.9 ± 0.8	12.9 ± 0.3
40/40/20	311 ± 4	8.5 ± 0.8	13.4 ± 0.2
35/35/30	317 ± 3	6.6 ± 0.5	12.1 ± 0.1

Data are given as means plus or minus the standard deviation.

properties of thermoplastics. Therefore, stiffer WP restricted the chain flexibility of the polymers, and hence, a further increase in the modulus of the blend composites was experienced.[7] A decrease in elongation at break as more WP was added to the blend was an indication of WP acting as defect points where stress cracking occurred easily. As more WP was added, a further decrease in the elongation at break was experienced because WP reduced the chain mobility of the polymers.[8,17,25,32,33] MAPP slightly improved the ability of EVA to handle stress, and the addition of WP to the MAPP/EVA blend further increased its tensile strength. This observation proved that there was an interaction between MAPP and EVA; in addition to this, there was also good compatibility between the stiffer WP and the MAPP/EVA blend. Wambua et al.[34] reported that plant fibers are, in general, suitable to reinforce plastics because of their relatively high strength and stiffness and low density. In comparison to the PP/EVA/WP blend composites,[17] the MAPP/EVA/WP blend composites had better mechanical properties. This was due to better interfacial interaction and compatibility between the WP and the MAPP/EVA blend, which was the result of the interactions between the different functional groups present in the system.

CONCLUSIONS

MAPP/EVA/WP polymer blend composites were prepared, and their morphology and thermal and mechanical properties were investigated. The MAPP and EVA in the blend were miscible because of the interaction between the functional groups in the two polymers. This observation was supported by the DMA, FTIR, SEM, and DSC results, which confirmed the compatibility of and interaction between the MAPP and EVA in the MAPP/EVA blend. The WP was found to be in contact with both MAPP and EVA in the MAPP/EVA/WP blend composites, and there was obvious interaction between the functional groups in WP, MAPP, and EVA. This improved the thermal stability of the second step in the thermal degradation of these blend composites, but the third step of the thermal degradation started at lower temperatures with an increase in WP content. Because of the interaction between the different phases, the presence of WP did not reduce the tensile properties of the blend, but it also did not really improve these properties. The interaction of EVA with MAPP and with WP caused a significant reduction in the EVA crystallinity and caused the EVA α transition, an indication of lamellar shear, to disappear.

References

1. Nygard, P.; Tanem, B. S.; Karisen, T.; Brachet, P.; Leinsvang, B. Compos Sci Technol 2008, 68, 3418.
2. Liu, H.; Wu, Q.; Han, G.; Yao. F.; Kojima, Y.; Suzuki, S. Compos A 2008, 39, 1891.
3. Bledzski, A. K.; Faruk, O. Compos Sci Technol 2004, 64, 693.
4. Yu, L.; Dean. K.; Li, L. Prog Polym Sci 2006, 31, 576.
5. Albano, C.; Reyes, J.; Ichazo, M.; Gonzalez, J.; Chipara, M. I. Polym Degrad Stab 2001, 73, 225.
6. Suarez, J. C. M.; Coutihno, F. M. B.; Sydentricker, T. H. Polym Test 2003, 22, 819.
7. Qui, W.; Zhang, F.; Endo, T.; Hirotsu, T. J Appl Polym Sci 2003, 87, 337.
8. Qui, W.; Endo, T.; Hirotsu, T. Eur Polym J 2006, 42, 1059.
9. Malavasic, T.; Musil, V. J. Therm Anal 1988, 34, 503.
10. Fonseca, C. A.; Harrison, I. R. Therm Acta 1998, 313, 37.
11. Huerta-Martinez, B. M.; Ramirez-Vargas, E.; Medellin-Rodrequez, F. J.; Garcia, R. C. Eur Polym J 2005, 41, 519.
12. Kim, S. J.; Shin, B. S.; Hong, J. L.; Cho, W. J.; Ha, C. S. Polymer 2001, 42, 4073.
13. Jansen, P.; Soares, B. G. Polym Degrad Stab 1996, 52, 95.
14. Menyhárd, A.; Varga, J. Eur Polym J 2006, 42, 3257.
15. Martins, C. G.; Larocca, N. M.; Paul, D. R.; Pessan, L. A. Polymer 2009, 50, 1743.
16. Si, X.; Guo. L.; Wang, Y.; Lau, K.-T. Compos Sci Technol 2008, 68, 2943.
17. Dikobe, D. G.; Luyt, A. S. eXPRESS Polym Lett 2009, 3, 190.
18. Mihaylova, M. D.; Nedkov, T. E.; Krestev, V. P.; Kresteva, M. N. Eur Polym J 2001, 37, 2177.
19. Gupta, A. K.; Ratnam, B. K.; Srinivasan, K. R. J Appl Polym Sci 1992, 45, 1303.
20. Jayanarayanan, K.; Thomas, S.; Joseph, K. Compos A 2008, 39, 164.
21. Oksman, K.; Clemons, C. J Appl Polym Sci 1998, 67, 1503.
22. Eroglu, M. Int J Sci Tech 2007, 2, 63.
23. Premphet, K.; Horanont, P. Polymer 2000, 41, 9283.
24. Ersoy, O. G.; Nugay, N. Polymer 2004, 45, 1243.
25. Uotila, R.; Hippi, U.; Paavola, S.; Seppala J. Polymer 2005, 46, 7923.
26. Seo, Y.; Kim, J.; Kim, K. U.; Kim, Y. C. Polymer 2000, 41, 2639.
27. Xanthos, M.; Young, M. W.; Biesenberger, J. A. Polym Eng Sci 1990, 30, 355.
28. Xu, J.; Xu, X.; Chen, L.; Feng, L.; Chen, W. Polymer 2001, 42, 3867.
29. Peeterbroeck, S.; Alexandre, M.; Jerome, R.; Dubois, P. Polym Degrad Stab 2005, 90, 288.
30. Joseph, P. V.; Joseph, K.; Thomas, S.; Pillai, C. K. S.; Prasad, V. S.; Groeninckx, G.; Sarkissova, M. Compos A 2003, 34, 253.
31. Duquesne, S.; Jama, C.; Le Bras, M.; Delobel, R.; Recourt, P.; Gloaguen, J. M. Compos Sci Technol 2003, 63, 1141.
32. Bledzki, A. K.; Gassan, J. Prog Polym Sci 1999, 24, 221.
33. Kim, H.-O.; Lee, B.-H.; Choi, S.-W.; Kim, S.; Kim, H. J. Compos A 2007, 38, 1473.
34. Wambua, P.; Ivens, J.; Verpoest, I. Compos Sci Technol 2003, 63, 1259.